STRUCTURAL OPTIMIZATION 1998 (in press)

Flaw identification in elastomechanics: BEM simulation with local and genetic optimization.

by

G.E. Stavroulakis and **H. Antes**

Institute of Applied Mechanics, Carolo Wilhelmina Technical University,
D–38023 Braunschweig, Germany

Keywords
nondestructive evaluation, flaw identification, boundary elements, genetic algorithms

Abstract

Single and multiple flaw identification problems are considered. Static and steady-state dynamic analysis of structures with flaw(s) is performed by the boundary element method. Inverse problems are formulated as output (i.e., measurement) error minimization problems and they are solved by numerical optimization techniques. As it is shown in this paper by means of numerical experiments, for elastostatic cases, an appropriate modeling of the structural analysis problem, a good choice of the error measure, and the use of established numerical optimization software are usually sufficient for the solution of the problem. Even multiple flaw identification is possible. Elastodynamic loadings lead to nonconvex problems which are solved here by means of global, genetic optimization algorithms.

1 Introduction

In this paper, the effectiveness of solving inverse, flaw detection problems in elastostatics and in harmonic elastodynamics is investigated by means of boundary element modeling for the direct problem, and of numerical optimization techniques for the solution of the inverse error minimization problem. The methodology is generally applicable to damage identification, flaw detection, and quality control of structures or structural elements.

Identification problems belong to the class of the so-called inverse problems, in the sense that a given model of a system is defined, and a set of input-output data for this system is available, but the values of the parameters, which are involved in the system, are unknown. The output error identification problem, which is considered here, is formulated as an optimization problem for the difference between the measured (or, for the examples presented in this paper, the computed) and the desired responses within the space of the variables which define the considered structure. The similarity of the problem with the ones arising in structural optimization is straightforward, if one identifies the error function with a cost function. In general, a certain structure is assumed for the defects, i.e., that they have the form of a crack, a circular hole or soft inclusion, a plastification zone, etc. The problem consists then in the determination of the parameters of the assumed defects. This approach uses in an optimal way the existing engineering experience about the failure mode of the sought structural component. Moreover, low sensitivity of the structural response with respect to the chosen flaw parameters and the fact that, especially for complicated flaw models, several values of these parameters may fit to the given measurements (thus the possible multiplicity of the solution) make the arising optimization problem ill-posed. In fact, the error function is, in general, nonconvex and, accordingly, the error minimization problem is a global optimization problem with several local minima. If appropriate scaling techniques (e.g., the use of another error measure) or the choice of other test loadings can not help to overcome this problem, appropriate global optimization algorithms must be employed (e.g., stochastic optimization, genetic algorithms, neural networks, etc.). Note that scaling helped also, in this case, to avoid the application of regularization techniques. More generally, the problem belongs to the class of mathematical programs with equilibrium constraints (see, e.g., Haslinger and Neitaanmäki (1988), Luo et. al. (1996)). In fact, an error function is minimized here with respect to the flaw parameters and with subsidiary conditions coming from the governing relations of the mechanical system. These relations are, for the cases considered in this paper, parametrized systems of linear equations (the nonlinearity being induced through the flaw parametrisation).

In this paper, a two–dimensional specimen is considered which contains a number of unknown circular defects. Each unknown defect has been parametrized by a certain number of parameters, e.g., the diameter of the circle and the coordinates of its center. It is assumed that certain boundary displacements or tractions can be measured for various external loadings.

The direct mechanical problem is solved numerically, for static and harmonic dynamic loadings, by the BEM method. The identification (inverse) problem is treated by numerical optimization techniques.

The significance of the area of flaw, defect and crack identification is underlined by the large number of recent publications. A brief citation of several works in this area will allow us to mention several directions of current research efforts. The list is indicative and by no means complete. Boundary element method techniques and classical minimization algorithms have been used for the identification of elliptic flaws by (Mitra and Das (1992) where steady heat conduction problems are examined. In (Tanaka and Masuda (1996)), the inverse elastostatic analysis problem is studied, where the shape of the unknown crack is identified by boundary measurements (see also (Nishimura and Kobayashi (1991)). Three dimensional flaw identification has been studied in (Mellings and Aliabadi (1994)). In (Tosaka et al. (1995)) the identification of elliptical defects in 2–D or spherical defects in 3–D problems is addressed. Here, the classical numerical minimization scheme is replaced by a Kalman filtering based iterative algorithm which reduces substantially the computational effort. The estimation of the position, size and elastic properties of an inclusion within a composite material from static analysis results has been studied in (Schnur and Zabaras (1992)), with a finite element modeling. Elastodynamic data are considered more advantageous for defect identification. The approach used in this paper, for the dynamic case, parallels the investigations of (Tanaka et al. (1991)) and (Weijiang and Chuntu (1996)). Genetic algorithms have been used for the solution of inverse fault detection in elastodynamics in (Kannal and Doyle (1997)) and Kalman filtering techniques in (Tosaka et al. (1995)). Neural networks have been used in several identification problems. Among others, crack identification using dynamic analysis data has been studied in (Oishi et al. (1995)), damage identification by using eigenmodal data and an inovatige scaling rule which enhances the performance of the neural network has been reported in (Yoshimura et al. (1996)) and the applications reported in (Yagawa and Okuda (1996)) are cited. Crack detection in elastostatics with unilateral contact effects along the crack sides has been studied in (Stavroulakis and Antes (1997)) by using BEM modeling and neural networks. Identification of a boundary crack in steady state elastodynamics has been studied by analogous techniques in (Stavroulakis and Antes (1998)). Recent applications in this quickly evolving area can be found in (Ingham and Wrobel (1997)).

The purpose of this work is twofold. First, by using numerical experimentation, the appearance of nonconvex (global) optimization problems in flaw identification is demonstrated. This effect is magnified in inverse elastodynamic problems. Logarithmic scaling of the error function or/and the simultaneous use of data from several excitation signals (several loading cases) usually make the problem tractable. Otherwise global optimization tools must be used. Genetic algorithm optimization is used in this paper. The second purpose of this work is the study of multiple flaw identification tasks. This problem is rarely addressed in the inverse problems literature. It seems that, at least during the present computer simulations, the identification of multiple flaws does not cause additional difficulty, except of the increased computational effort which is due to the larger number of parameters. Moreover, the following simple strategy works satisfactorily. Assume that the exact number of flaws is unknown, but the maximum number of them in a given problem can be estimated. Then, instead of solving complicated zero-one optimization problems one may try a classical multiple flaw identification procedure by using the maximum number of expected flaws. Flaws with “zero” values in the results do not actually exist in the examined structure.

The paper is organized as follows. The BEM formulations for the solution of the direct elastostatic and elastodynamic, steady state problem, are briefly outlined in section two. The inverse problem formulation is described in section three, where the used error measures is given. The application of local and global (genetic) optimization is briefly described in section four. Results of numerical experiments are reported and discussed in the last section of this paper.

2 BEM Structural Analysis Modeling

2.1 Elastostatics

The BEM formulation for the elastostatic problem is outlined here. More details can be found in standard textbooks (see, among others, Brebbia and Dominguez (1989) or Antes and Panagiotopoulos (1992)).

Let us consider the equations of equilibrium, written in a Cartesian coordinate system, for each point x of an elastic body which occupies the area Ω with the boundary Γ :

$$\sigma_{ij,j}(x,t) + p_i(x,t) = 0, x \in \Omega. \tag{1}$$

Here σ_{ij} is the stress tensor and p_i is the volume force vector. Moreover i, j run over the values 1..3 for three dimensional problems (resp. the values 1...2 for two dimensional problems) and the usual Einstein's summation assumption for repeated indices is adopted.

By using the reciprocal theorem of Green and adequate fundamental solutions and by assuming that only boundary loadings $T_i(x)$ are applied on the structure, one may obtain the boundary integral equation of the system at each point $\xi \in \Omega$:

$$d(\xi)u_j(\xi) = \int_\Gamma \left[T_i(x)u_i^{j*}(x,\xi) - u_i(x)T_i^{j*}(x,\xi)\right] d\Gamma_x. \tag{2}$$

Here ξ and x are the points on the boundary Γ or in the body Ω, u (resp. T) is the displacement (resp. the traction) vector, $u^*(x,\xi)$ (resp. $T^*(x,\xi)$) denotes the fundamental solution (resp. its normal derivative $u^*_{,n}$ on the boundary) and the jump factor $d(\xi)$ is calculated as usual in the BEM (e.g., $d(\xi) = 0.5$ for a smooth part of the boundary).

Finally, evaluating equation (2) at certain points ξ, the so–called collocation points, using appropriate shape functions in the discretized boundary, i.e., in the boundary elements, and applying adequate quadrature formulae for the numerical integration, one gets the following system of linear equations:

$$\mathbf{Hu} = \mathbf{Gt}. \tag{3}$$

The dimension of the element traction vector $\mathbf{t}$ depends on the kind of the used boundary element shape functions. For simplicity, let us consider a two–dimensional structure which is discretized by m boundary elements with a total of n boundary nodes. The quadratic elements used here have three nodes in each element. Thus, in (3), since the displacements are assumed to be continuous, $\mathbf{u}$ is a vector containing $2n$ nodal boundary displacements, while, since the traction may be discontinuous at the ends of the elements, $\mathbf{t}$ is a vector containing $3m$ nodal boundary tractions. The nonsymmetric matrices $\mathbf{H}$ and $\mathbf{G}$ have dimensions $2n \times 2n$ and $2n \times 6m$, respectively, and have the mechanical meaning of generalized influence matrices.

From the boundary conditions of the system, complementary terms of the boundary displacements or tractions are given. This information is used for the re–arrangement of the system (3). Finally, the calculation of the remaining unknown boundary displacements and tractions, i.e., of the $2n$–dimensional vector $\mathbf{x}$, is obtained from the solution of a nonsymmetric system of equations:

$$\mathbf{Ax} = \mathbf{b}. \tag{4}$$

In this concise formulation the vector $\mathbf{x}$ is made up of all unknown elements of the displacement vector $\mathbf{u}$ and the traction vector $\mathbf{t}$, while the right hand side term vector $\mathbf{b}$ contains the influence of all given boundary tractions and displacements (i.e., the given complementary set of elements of $\mathbf{u}$, $\mathbf{t}$ multiplied by the corresponding rows of the influence matrices in (3)).

2.2 Harmonic Elastodynamics

The formulation of the reduced elastodynamics equations is outlined here (see, among others, (Antes, 1988) and (Antes and Panagiotopoulos 1992) for more details). Let us consider the equations of motion, written in a Cartesian coordinate system, for each point x of an elastic body:

$$\sigma_{ij,j}(x,t) - \rho(x)\ddot{u}_i(x,t) + p_i(x,t) = 0, x \in \Omega. \tag{5}$$

Here ρ is the mass density of the body. On the assumptions of linear elastic material behaviour and of small amplitude vibrations, i.e., a small displacements and deformations theory, equation (5) takes the form:

$$\left(c_1^2(x) - c_2^2(x)\right) u_{j,ji}(x,t) + c_2^2(x) u_{i,jj}(x,t) - \ddot{u}_i(x,t) + \frac{p_i(x,t)}{\rho(x)} = 0, x \in \Omega. \tag{6}$$

In (6), c_1 is the dilatational (or pressure) and c_2 is the distortional (or shear) wave propagation velocity. For plane strain two dimensional isotropic elasticity applications, c_1 , c_2 are related with the elasticity modulus E and the Poisson's ratio ν as follows:

$$c_1^2 = c_p^2 = \frac{E(1-\nu)}{\rho(1+\nu)(1-2\nu)}, c_2^2 = c_s^2 = \frac{E}{2\rho(1+\nu)}. \tag{7}$$

A linear elastic, homogeneous and isotropic material law is assumed hereafter.

Further, let us assume that all elastodynamic quantities of the studied problem are time harmonic. Thus, for a given frequency ω the excitation takes the form $p_i(x,t) = \widehat{p}_i(x)e^{i\omega t}$ with $i = \sqrt{-1}$. Accordingly, the response of the system is harmonic as well, thus we use the Ansatz $u_i(x,t) = \widehat{u}_i(x)e^{i\omega t}$. Under this transformation, the time dependent equations of motion (5)-(7) take the following frequency dependent form:

$$\left(c_1^2(x) - c_2^2(x)\right) \widehat{u}_{j,ji}(x) + c_2^2(x)\widehat{u}_{i,jj}(x) + \omega^2 \widehat{u}_i(x) + \frac{\widehat{p}_i(x)}{\rho(x)} = 0, x \in \Omega. \tag{8}$$

By using the reciprocal theorem of Green and adequate fundamental solutions and by assuming that only boundary excitations are applied on the structure, one may obtain the following boundary integral equation :

$$d(\xi)\hat{u}(\xi) = \int_\Gamma \left[\widehat{p}(x)\widehat{u}^*(x,\xi;\kappa_1,\kappa_2) - \widehat{u}(x)\widehat{p}^*(x,\xi;\kappa_1,\kappa_2)\right] d\Gamma. \tag{9}$$

Here $\kappa_1 = \frac{\omega}{c_1}, \kappa_2 = \frac{\omega}{c_2}$, are the wave numbers, ξ and x are the points on the boundary Γ or in the body Ω, $\widehat{u}^*(x,\xi;\kappa_1,\kappa_2)$ (resp. $\widehat{p}^*(x,\xi;\kappa_1,\kappa_2)$) denotes the fundamental solution (resp. its normal derivative $\hat{u}^*_{,n}$ on the boundary) and $d(\xi)$ is the jump factor.

After appropriate point collocation and boundary element discretisation one gets the discretized form of (9):

$$\mathbf{H}(\kappa_1,\kappa_2)\mathbf{u} = \mathbf{G}(\kappa_1,\kappa_2)\mathbf{t}, \tag{10}$$

where $\mathbf{u}$ (resp. $\mathbf{t}$) denotes the boundary nodal displacement (resp. boundary traction) vector and the influence matrices $\mathbf{H},\mathbf{G}$ depend on the assumed excitation frequency ω.

Further processing of (10), i.e., taking into account the boundary conditions of the structure, separating known and unknown elements of vectors $\mathbf{u}$ and $\mathbf{t}$ according to the boundary conditions of the structure, forming the system of equations etc, follows the classical techniques in the BEM (analogously to the previous static case). Finally, one gets the system of equations:

$$\mathbf{A}(\omega)\mathbf{x}(\omega) = \mathbf{b}(\omega), \tag{11}$$

with solution denoted by $\mathbf{x}(\omega,\mathbf{b})$ for a given frequency ω and a given 'loading' vector $\mathbf{b}$.

2.3 Flaw parametrization aspects

From the structure of the BEM equations (3) (resp. (10)) and from the expression of the fundamental solutions (which can be found, for instance, in Antes and Panagiotopoulos (1992)), one may observe that the matrices $\mathbf{H}$ and $\mathbf{G}$ (resp. $\mathbf{H}(\kappa_1,\kappa_2)$ and $\mathbf{G}(\kappa_1,\kappa_2)$) depend on the coordinates of the collocation points and the coordinates of all points along the boundary which appear, after discretization, within the integration terms. A subset of these nodal coordinates model the boundaries of the internal, unknown flaws. These values, appropriately grouped to reduce the dimensionality of the problem, will be used here as the unknowns of the inverse (flaw identification) problem.

It is obvious that the above relation, i.e., between the boundary nodal coordinates and the solution of the arising system of linear equations for a given loading and boundary conditions is nonlinear.

Moreover, analogously to the finite element method, one may differentiate the equations (3) or (10) in order to get sensitivity relations (see, e.g., Bruzynsky et al. (1996, 1997)). Nevertheless, one should take into account that higher order singularities arise in this course and appropriate attention must be paid during the numerical evaluation of the arising integrals.

In this paper, gradient and higher order information, when needed, are approximated at the numerical optimization level. Thus, only the values of the solution of the structural analysis problem for a given value of the fault parameter are used. The sensitivity analysis would therefore enhance the numerical effectiveness of the algorithms.

Let us consider a given number of parameters $\mathbf{z} = [z_1, \ldots, z_m]^T$ which fully characterize the expected flaws in the structure. For instance, assume that cyclical flaws are expected to be found in the structure, or the existing defects can be modelled by such cyclical flaws. Then, the coordinates of the centers of the flaws and their diameters constitute a set of appropriate parameters for the considered inverse problem.

In view of the previously introduced parametrization, all matrices $\mathbf{H}$, $\mathbf{G}$ in equation (3) (resp. in (9)) depend on the value of $\mathbf{z}$, i.e., we have $\mathbf{H}(\mathbf{z})$, $\mathbf{G}(\mathbf{z})$ (resp. $\mathbf{H}(\kappa_1, \kappa_2, \mathbf{z})$, $\mathbf{G}(\kappa_1, \kappa_2, \mathbf{z})$). Accordingly, after the solution of the direct problem (cf. (4), resp. (10)) one gets parameter dependent values of the boundary displacements and tractions. Finally, the response of the structural system, i.e., the unknown boundary displacements and tractions which are grouped together into vector $\mathbf{x}$, as it is usual in boundary element methods, depends on the flaw parameters $\mathbf{z}$, on the applied loading $\mathbf{b}$ and, for the elastodynamic case, on the excitation frequency ω. Concisely, we denote this dependence by $\mathbf{x}(\mathbf{z}, \mathbf{b})$ (resp. $\mathbf{x}(\mathbf{z}, \omega, \mathbf{b})$).

3 Inverse Problem Formulation

An output error minimization problem is formulated and solved. The elastodynamic identification problem is described in this section, since the relations of the elastostatic problem can be obtained by simply rejecting the frequency dependence (all ω's are deleted).

Let a structure with unknown flaws be subjected to a number of external loadings $\mathbf{b}^l$, $l = 1, \ldots, l_1$, with corresponding frequencies ω^m, $m = 1, \ldots, m_1$. Let the measured responses of the structure be denoted by $\mathbf{x_0}(\omega^m, \mathbf{b}^l)$, for the loading ω^m, $\mathbf{b}^l$. Let, moreover, a model of the same structure be constructed which contains a number of test flaws parametrized by $\mathbf{z}$. The corresponding response of the structure, which is subjected to the same loading ω^m, $\mathbf{b}^l$, is denoted by $\mathbf{x}(\mathbf{z}, \omega^m, \mathbf{b}^l)$.

The inverse problem is formulated as a minimization problem for a scalar performance error function:

$$e(\mathbf{z}) = \sum_{l=1}^{l_1} \sum_{m=1}^{m_1} \left(\|\mathbf{x}(\mathbf{z}, \omega^m, \mathbf{b}^l) - \mathbf{x}_0(\omega^m, \mathbf{b}^l)\| \right) \tag{12}$$

Here $\|\cdot\|$ is an appropriate norm. Usually, the L^2 norm is adopted (least square identification). Here, summation over all available loading cases and all excitation frequencies forms a compromising gain function. Other choices can also be considered.

Due to the nonlinear nature of the parametrized mapping $\mathbf{z} \to \mathbf{x}(\cdot, \omega, \mathbf{b})$, the composite function $e(\mathbf{x}(\mathbf{z})$ is, in general, non-convex. As it is also shown in the numerical experiments, the nonconvexity effect is more severe in elastodynamic problems.

In the numerical experiments, the use of the following logarithmic transformation has been proved beneficially:

$$e'(\mathbf{z}) = \log(e(\mathbf{z}) + \epsilon), \tag{13}$$

where ϵ is a small positive constant, which prevents the appearance of a $-\infty$ value in e' ($\epsilon = 0.1 * 10^{-5}$ is used here).

Moreover, a restricted number of measurements (i.e., number of elements of $\mathbf{x}$) can be used in the previous problems. In general, the performance of the identification problem depends on the choice of the response values which are used (number and position of measuring points) and on the considered loading case(s)(cf., for static problems, Banan et al., (1994)).

Obviously, the solution of a minimization problem with the error function (12) leads to an estimate of the existing flaws. The quality of this estimate depends on the assumed parametrization of the flaws and the numerical accuracy of the mechanical modeling. The latter point is facilitated here by the use of the boundary element method. In an ideal situation, the value of the error function $e(\mathbf{z})$ should be equal to zero for a correct solution of the identification problem, i.e., the minimum of the goal function in the previously described optimization problem should be equal to zero.

4 Numerical solution of the inverse problem

4.1 Local optimization approach

The optimization problem with respect to the functions (12), (13) has been solved by means of a general purpose numerical optimization program.

The code *E04UCF* of the *NAG* library is used. Only function evaluations are required from this program. It is an implementation of the sequential quadratic programming method where, internally, the Hessian matrix is approximated by means of finite difference approximations. Moreover, significant iterations in this procedure are called major steps while all other iterations which are used to correct the local quadratic approximation of the function are termed minor steps.

In principle, a code which uses also higher order information of the error function (e.g., gradients) would lead to a higher numerical effectiveness. Nevertheless, in that case, a sensitivity analysis of the structural problem with respect to the flaw parameters has to be performed.

More sophisticated numerical optimization techniques can also be applied (for instance, see the Levenberg-Marquardt method used in (Schnur and Zabaras (1992), the regularization techniques, (Baumeister (1993)), (Manniatty and Zabaras (1994), (Kaplan and Tichatchke (1994) etc.).

4.2 Global, genetic algorithm approach

The nonconvex optimization problem which arises during the inverse flaw identification problem may have several local minima, as it has been shown by means of numerical examples in the next sections. Thus, a global optimization method is required for its numerical solution. In this paper, a genetic algorithm is used.

In the framework of the genetic optimization, the set of unknown variables of the problem (i.e., its flaw characteristics, its phenotype) are encoded as a chain of binary variables (cf., chromosomes). Furthermore, due to the stochastic nature of this approach, a population of test flaws is assumed. For each set of values of the flaw variables, the error function $e(\mathbf{z})$ is calculated. Each of this set constitutes an individual in this population. In accordance with the terminology used in genetic optimization, the minimization problem is transformed into a maximization problem. Thus, instead of an error function, a fitness function arises, whose maximum is sought.

The procedure is further partially inspired by the Darwin's rule of survival through natural selection. In the *selection* step individuals with better fitness values are given a higher probability to be mated and to inherit their characteristics to the next generation. A *crossover* operator permits parts of the encoding string of the parents to be exchanged within the reproduction step. Finally, arbitrary parts of the information are changed at random (*mutation*) during the creation of the new generation. Sometimes, very good individuals are allowed to pass through the whole procedure unchanged (*elitism*), i.e., they are copied as they are in the next generation.

Some technical details of the application, in particular, the points that affected the numerical performance of the examined examples, are briefly addressed here. More information may be found in the specialized literature (for instance, see Goldberg (1989)). In particular, a short description of a genetic algorithm approach to shape optimization appeared recently in this journal (Haslinger and Jedelský (1996), pp. 261–263).

A first implementation point concerns the transformation of the error minimization problem to a fitness maximization one. The error measure $e(\mathbf{z})$ of the flaw identification problem takes the role of the environmental factor in a genetic population evolving in nature. As fitness function, the following objective can be used:

$$f_1(\mathbf{z}) = \begin{cases} \frac{1}{e(\mathbf{z})} & \text{for} \quad e(\mathbf{z}) \not= 0, \\ M & \text{for} \quad e(\mathbf{z}) = 0, \end{cases} \tag{14}$$

where M is a large positive number. Another variant has also been tested (see, Goldberg (1989), p. 76):

$$f_2(\mathbf{z}) = \begin{cases} M - e(\mathbf{z}) & \text{for} \quad e(\mathbf{z}) < M, \\ 0 & \text{for} \quad e(\mathbf{z}) = M. \end{cases} \tag{15}$$

Moreover, the encoding strategy should be chosen with care. As it transforms the continuous variable optimization problem (where the flaw parameters $\mathbf{z}$ are the unknown variables) into a discrete one, the number of, e.g., binary codes used for the chromosome mapping of each variable dictates the accuracy of the results. A fine discretization of the variables space which requires larger binary codes leads to a higher accuracy, but it is also connected with a higher computational cost.

It should be mentioned that genetic algorithms are general purpose, probabilistic optimization methods which tackle directly a multi-extremum nonconvex (global) optimization problem. Only the value of the function is required, thus the procedure is applicable to nondifferentiable problems as well (cf., Hajela (1990)). Even discontinuous functions or optimization problems with discrete variables may be considered (cf., recent engineering applications described, among others, in Rajeev and Krishnamoorthy (1992, 1997), Grierson and Pak (1993), Cai and Thierauf (1993), Huang and Arora (1997). One should mention, however, that there are also deficiencies in this approach. First, due to their generality, generic algorithms require enough computer time. Fortunately, they permit a high degree of parallelization (see, e.g., the results in this direction reported in (Adeli and Kumar (1995)). Moreover, since in a genetic process all available information is stored in the genetic information of the living generation, a fairly large amount of information which is produced at the previous iterative steps of the procedure (the several function evaluations) is being lost.

A number of complicated problems in structural optimization have recently been solved by using genetic algorithms. For instance, optimal design of laminated composites including buckling constraints is studied in Le

Riche and Haftka (1993). In this paper, an alternative three–alphabet encoding is used, which is more appropriate for the considered application. Optimal shape design problems are treated, among others, in Haslinger and Jedelský (1996) and in Annicchiarico and Cerrolaza (1997). Discrete optimization problems in structural analysis has been considered in (Rajeev and Krishnamoorthy (1992)), (Cai and Thierauf (1993)) and (Huang and Arora (1997)). An application on form finding problems in slack cable networks and similar structures which undergo large displacements has been done in (Hartmann (1996)), where the genetic algorithm scheme has been used for the solution of the potential energy minimization problem.

In the area of inverse problems in mechanics, Doyle presented in a number of papers an approach for the localization of defects and flaws in structures. First, he uses dynamic results which are produced by a spectral finite element program in order to estimate the unknown excitation loading. Then, by making assumptions on the position and shape of the flaw, he uses as an error measure the difference between two predicted loadings, which are produced by two different assumptions about the unknown defect. Obviously, if this difference is zero, the assumption is correct and the defect is correctly identified. Details of this application can be found in Doyle (1994), Kannal and Doyle (1997) and in the references given therein.

5 Numerical Examples

5.1 Static loadings

A plane strain plate with several holes (flaws) is considered. For the BEM discretization, the boundaries of the plate are discretized by means of quadratic boundary elements. The whole procedure is automatically done by the computer. Only the outer dimensions of the plate, the position and the length of the holes and the discretisation parameters need to be given.

The material constants are the shear modulus G=100000.0 and the Poisson's ratio 0.3. The external dimensions of the plate are 10.00×10.00, all in compatible units.

In all examples presented here, the external boundary is discretized by means of 20 boundary elements (i.e., a total of 40 nodes) and each hole is discretized by means of 5 boundary elements (i.e., additional 10 nodes for each flaw). Moreover, the right hand side external boundary (bc in Fig. 1) is fixed and the loading is applied on the left hand side external boundary (ad in Fig. 1).

A representative example of a static solution for uniform external tractions equal to 1000.0, in both the horizontal Ox and in the vertical Oy coordinate direction, is given in Fig. 2. Three circular holes are considered. Their centres are at the positions $(1.5, 1.5)$, $(5.0, 7.0)$ and $(7.5, 5.0)$. The diameters are equal to (0.5), (2.0) and (1.1), respectively. Note that relatively large holes are considered here in order to facilitate the graphical representation of the deformed configuration. Nevertheless, in the identification problems solved later, considerably smaller flaws are considered.

After a parametric investigation, the error function $e(\mathbf{z})$ of (12) and the logarithmic error $e'(\mathbf{z})$ of (13) are plotted in Figs 3a,b, respectively. The known flaw is a cyclical hole of diameter equal to 0.1, centred at the point $(5.0, 5.0)$. Comparison flaws have been calculated at all vertices of an orthogonal net with centre points at $x \in (1.0, 9.0)$, $y \in (1.0, 9.0)$, and steps equal to 1.0.

Let us now consider the identification problem for the position of the centre of two cyclical flaws, with centres at $(5.0, 5.0)$ and $(7.0, 5.0)$ and of diameter equal to 0.1. From starting points equal to $(2.0, 7.0)$ and $(5.0, 3.0)$ and from an initial test diameter value equal to 0.3, the SQP optimization algorithm converges to the correct solution after 38 major and 51 minor iterations. The history of all iterative values for the centre of the first flaw, the centre of the second flaw, and the two flaw diameters, for all function evaluations, is mapped in Figs. 4a,b and c, respectively. The history of the error function values e' versus the major (significant) iterations of the algorithm is given in Fig. 4.d.

Identification of one flaw, by starting from the assumption that two flaws exist, is demonstrated in Figs. 5a–d. Here, two cyclical flaws of initial centre positions equal to $(7.0, 2.0)$ and $(2.0, 4.0)$ and of diameters equal to (0.4) and (0.02) are assumed. Finally, the one actually existing flaw at centre $(5.0, 5.0)$ with diameter equal to (0.1) is identified. The centre values of the second flaw converge to the arbitrary values $(1.58, 3.90)$. Nevertheless, its diameter converges to a small number equal to 0.015, which has been set to be the lower limit allowed for this value in the optimization problem.

The latter case, where some of the assummed flaws do not exist, is shown in the results of two more tests. In both cases, a circular defect with centre at $(5.0, 5.0)$ and with diameter equal to (0.1) is asumed.

TEST 1	**Flaw 1**		**Flaw 2**	
	Initial	**Final**	**Initial**	**Final**
x-coordinate	2.0	4.5	7.0	5.93
y-coordinate	2.0	2.09	7.0	5.39
diameter	0.3	0.05	0.3	0.09

TEST 2	**Flaw 1**		**Flaw 2**	
	Initial	**Final**	**Initial**	**Final**
x-coordinate	2.0	4.55	2.0	5.13
y-coordinate	2.0	2.49	9.0	4.82
diameter	0.3	0.05	0.5	0.1018

TEST 3	**Flaw 1**		**Flaw 2**	
	Initial	**Final**	**Initial**	**Final**
x-coordinate	2.0	4.98	2.0	1.618
y-coordinate	2.0	4.94	9.0	3.91
diameter	1.0	0.1053	1.0	0.051

Without presenting more numerical values we would like to conclude that:

- Using static loadings, the BEM- numerical optimization approach to the static, inverse flaw detection problem works satisfactorily. All presented examples require less than five minutes computing time on an *IBM RISC/6000* Workstation, with no attempt on code optimization.

- The logarithmic error function (13) leads to better convergence results than the simple Euclidean error measure (12). Regularization was not needed in this approach.

- If zero dimension flaws (e.g., circles of zero diameter) are expected to occur in the inverse problem, two strategies may be adopted:

  1. either, a lower limit ("numerical zero") is posed on the numerical optimization routine and one assummes that variables which have reached this limit lead to flaws with negligible influence on the structural response,
  2. or, for values lower than a small limit, the corresponding flaw is assumed to disappear, thus, it is not longer included in the BEM model.

  Usually, both tricks work for the majority of the tested cases. The results may depend on the initial values, but, they give usually a reasonable estimate of the existing defect. Nevertheless, the second strategy, which has been automatically incorporated in the computer program, has caused convergence problems in some examples. The reason is that the discontinuous change of the mechanical model lead to discontinuities in the arising error function at that point. Some kind of gradual reduction schemes have to be adopted for this case, which will be a subject of further investigations.

5.2 Dynamic loadings

Let us assume the same plate considered in Fig. 2, but this time subjected to a harmonic dynamic loading. For frequency values equal to $\omega = 5.0$, 10.0, 15.0 and 20.0, the corresponding vibration modes, magnified by a factor of 10.0, are shown in Fig. 6.

A parametric investigation is first performed, similarly to the static case. A cyclical flaw of diameter 0.50 is placed at several positions in the plate. The response is compared with the one of a same flaw at the place $(4.0, 4.0)$. The error function (12) and the logarithmic version (13) are plotted in Fig. 7a and b. All four previously given frequencies are considered.

The appearance of nonconvex error functions, which possibly have local minima, seems to be inherent in elastodynamic flaw identification problems. It depends on the excitation frequency, the loading and the measurement points. The combined use of the measurements of several excitation frequencies, as it has been suggested in (12), and the use of the logarithmic scaling of (13) make the problem more tractable. Nevertheless, this scaling does not work satisfactorily in all cases. Moreover, technological restrictions posed by the existent experimental devices should be taken into account.

Due to space limitations only a very small subset of the parametric investigation results can be presented here. Using only one excitation frequency at a time, with loading as previously in both Ox and Oy directions at the left hand side of the plate, leads to the results plotted in Figs. 8a–d. The effect of using different excitation loadings (e.g., only in the horizontal - Ox - or in the vertical - Oy - direction) and of using measurements of the boundary displacements in only one direction is shown in Figs. 9a–d. These effects are also present in the multiple flaw detection problem, where due to the higher dimension of the problem an analogous graphical representation is difficult.

In view of all these difficulties, a global optimization algorithm is the only robust method for the numerical solution of the problem. The local optimization algorithm used for the static case can also applied. Nevertheless, as it should have been expected, the results depend strongly on the starting iteration point. Moreover, termination at a local minimum of the nonconvex error function, which is not the sought solution of the inverse problem, is not rare.

A *FORTRAN* genetic algorithm optimization program (see Carroll (1996)) has been used here. The more effective choice of the parameters for the considered elastodynamic identification problem with the fitness function of (14), combined with the logarithmic error measure of (13) has been:

Variable	Effective Values
population size	5
crossover probability	0.5
creep mutation probability	0.04
jump mutation probability	0.20

A typical plot of the initial population (i.e., the starting guesses of the center point of the flaw) and the final population (i.e., the solution of the problem) is shown in Fig. 10a. The history of the maximum and of the mean value of the fitness function among all members of a population for all generations (i.e., the iterations of the algorithm) is shown in Fig. 10b. It should be mentioned that the relatively large deviation shown in Fig. 10b between the maximum and the mean value of the fitness function within the members of one generation does not correspond to a large inaccuracy of the results, due to the logarithmic nature of the fitness function.

Simultaneous position and size identification can also be done. A sample set of results (after 200 generations) is given in the following table:

TEST 4	**Real**	**Calculated**	
		Best Element	**Average**
x-coordinate	4.0	3.9606	5.59
y-coordinate	4.0	4.0236	4.74
diameter	0.5	0.4968	0.52
error e'		13.914	8.16

The choice of the parameters of the genetic algorithm influences the results. Unfortunatelly no clear picture can be drawn from the numerical experiments concerning the best choise of the parameters involved in the genetic optimization algorithm, a fact that is well known in the specialized literature (see, for instance, Mitchell (1996), p. 175). The variables used here led to satisfactory results for the considered application. For example, the influence of the size of the population is shown in the next results (they concern the identification of the coordinates of the center of one cyclical flaw of diameter equal to 0.5, and they are obtained after 200 generations):

TEST 5	**Population**	**Size = 5**
	Best Element	**Average**
x-coordinate	4.02	4.02
y-coordinate	3.96	3.89
error e'	13.88	12.50

TEST 6	Population Best Element	Size = 10 Average
x-coordinate	4.02	4.11
y-coordinate	4.02	3.68
error e'	14.97	11.42

TEST 7	Population Best Element	Size = 15 Average
x-coordinate	3.96	3.93
y-coordinate	3.96	3.87
e'	13.93	11.06

It is observed that reasonable results can be calculatedal in this application with small population sizes.

One typical run of 200 generations, which are multiplied by a population equal to 5 and result in an equivalent of 1000 solutions of the structural problem, requires about one hour time on a *SGI PowerChallenge* 12-processor computer system. Nevertheless, parallelization is not used by our preliminary computer code.

6 Conclusions

A numerical investigation of some inverse flaw detection problems is presented. For static excitations a logarithmic scaling of the error function has helped classical, local optimization algorithms to solve the inverse problem. For harmonic dynamic excitations the inverse problem is usually nonconvex and requires global optimization algorithms. A careful modeling may also effectively tackle multiple flaw identification problems.

One should note that the model for flaw detection, which has been used here, is much more economical to implement than damage identification methods which are based on damage mechanics' concepts. This is especially true if it is combined with the boundary element modelling, due to the fact that the meshing and remeshing requirements of this method are not high (in fact, only the boundary of the structure and of the flaws is discretized). An extension to identification problems concerning soft or hard inclusions is in principle possible, following the same procedure and multi-region boundary element modelling. One should nevertheless accept the limitations of this approach with respect to a more general one based on damage and plasticity modelling of the defects. On the other hand flaw identification may approximate, in some extend, crack detection problems (cf., the penny shape crack approach).

Further work in this direction should consider optimization of the performance of the numerical algorithms, or use of more complicated ones for the solution of the inverse problem. This is especially true for the nonconvex case, since the genetic algorithm approach, although it is a general purpose method, is not usually the more economical one. Thus, an extensive parametrical investigation, especially in the dynamic problem, is unfortunatelly combined with the use of enormous computer resources. Finally, the examination should extended into real life nondestructive evaluation problems by considering issues like technological restrictions, measurement errors etc. In view of the uncertainties and of the high cost of the classical optimization tools, the examination of soft computing tools (including, for this case, neural network and Kalman filter based approaches) may provide an interesting alternative.

Acknowledgements

The support of the European Union in the form of a TMR Research Grant (No. ERBFMBICT960987) is greatfully acknowledged.

References

Adeli, H.; Kumar, S. 1995: Distributed genetic algorithm for structural optimization. *ASCE J. of Aerospace Engineering*, **8(3)**, 156–163.

Annicchiarico, W.; Cerrolaza, M. 1997: Structural shape optimization using genetic algorithms. In: *Boundary Elements XIX*, Eds. M. marchetti, C.A. Brebbia and M.H. Aliabadi, pp. 399–408, Southampton: Computational Mechanics Publications.

Antes, H. 1988: *Anwendungen der Methode der Randelemente in der Elastodynamik und der Fluiddynamik.* B.G. Teubner Verlag, Stuttgart.

Antes, H.; Panagiotopoulos, P.D. 1992: *An integral equation approach to the static and dynamic contact problems. Equality and inequality methods.* Boston, Basel, Stuttgart: Birkhäuser Verlag.

Banan Mo.R.; Banan Ma.R.; Hjelmstad K.D. 1994: Parameter estimation of structures from static response. I: computational aspects. *ASCE J. Structural Engineering* **120(11)**, 3243–3258.

Baumeister, J. 1993: Identification of parameters, ill–posedness and adaptive systems. In: H.G. Natke, G.R. Tomlinson, J.T.P. Yao (eds), *Safety evaluation based in identification approaches*, pp. 148–165, Vieweg Verlag, Braunschweig, Wiesbaden.

Bezerra, L.M.; Saigal, S. 1993: A boundary element formulation for the inverse elastostatics problem (iesp) of flaw detection. *International Journal for Numerical Methods in Engineering*, **36** 2189–2202.
Brebbia, C.A.; Dominguez, J. 1989: *Boundary Elements. An introductory course.* Computational Mechanics Publications and McGraw–Hill Book Co..
Burczynski, T.; Kane, J.H.; Balakrishna, C. 1995: Shape design sensitivity analysis via material derivative adjoint variable technique for 3–d and 2–d curved boundary elements. *International Journal for Numerical Methods in Engineering*, **38** 2839–2866.
Burczynski, T.; Kuhn, G.; Antes, H.; Nowakowski, M. 1997: Boundary element formulation of shape sensitivity analysis for defect identification in free vibration problem. *Engineering Analysis with Boundary Elements*, **19(2)** 167–176.
Cai, J.; Thierauf, G. 1993: Discrete structural optimization using evolution strategies. In: *Neural Networks and Combinatorial Optimization in Civil and Structural Engineering*, Eds. B.H.V. topping and A.I. Khan, pp. 95–100, Edinburgh: Civil-Comp. Press.
Carroll, D.L. 1996: Chemical laser modeling with genetic algorithms. *AIAA Journal*, **34(2)** 338–346.
GA code available at $< http://www.staff.uiuc.edu/\tilde{}carroll/ga.html >$.
Dominguez, J. 1993: *Boundary elements in dynamics.* Computational Mechanics Publications, Shouthampton, Boston and Elsevier Applied Science, London, New York.
Doyle, J.F. 1994: A genetic algorithm for determining the location of structural impacts. *Experimental Mechanics*, 37–44.
Goldberg, D.E. 1989: *Genetic algorithms in search, optimization, and machine learning.* Reading, Massachussets etc: Addison–Wesley Publ.
Grierson, D.E.; Pak, W.H. 1993: Optimal sizing, geometrical and topological design using a genetic algorithm. *Structural Optimization*, **6**, 151-159.
Hajela, P. 1990: Genetic Search. An approach to the nonconvex optimization problem. *AIAA Journal*, **28**, 1205–1210.
Hartmann, Ch. 1996: *"Simulierte Evolution": Ein Lösungsansatz für Formfindungsprobleme ?.* PhD Dissertation, Munich: Technical University.
Haslinger, J.; Neittaanmäki, P. 1988: *Finite element approximation of optimal shape design: theory and applications.* Chichester: John Wiley and Sons.
Haslinger, J.; Jedelský , D. 1996: Genetic algorithms and fictitious domain based approaches in shape optimization. *Structural Optimization*, **12**, 257–264.
Huang, M.-W.; Arora, J.S. 1997: Optimal design with discrete variables:

some numerical experiments. *Intern. J. for Num. Meths in Engng.*, **40**, 165–188.
Ingham, D.B.; Wrobel, L.C. (eds.) 1997: *Boundary integral formulations for inverse analysis.* Southampton: Computational Mechanics Publications.
Kannal, L.E.; Doyle, J.F. 1997: Combining spectral super-elements, genetic algorithms, and massive parallelism for computationally efficient flaw detection in complex structures. *Computational Mechanics*, **20**, 67–74.
Kaplan, A.; Tichatchke, R. 1994: *Stable methods for ill–posed variational problems.* Berlin: Akademie Verlag.
Luo, Z. Q.; Pang, J. S.; Ralph, D. 1996: *Mathematical programs with equilibrium constraints*, Cambridge: Cambridge University Press.
Maniatty, A.M.; Zabaras, N.J. 1994: Investigation of regularization parameters and error estimating in inverse elasticity problems. *International Journal for Numerical Methods in Engineering*, **37** 1039–1052.
Mellings S.C.; Aliabadi M.H. 1994: Three dimensional flaw identification using sensitivity analysis. In: *Boundary Element Method XVI*, Ed. C.A. Brebbia, pp. 149–156, Computational Mechanics Publications, Southampton, Boston.
Mitra, A.K.; Das, S. 1992: Solution of inverse problems by using the boundary element method. In: *Boundary Element Technology VII*, Eds. C.A. Brebbia, M.S. Ingber, pp. 721–731, Computational Mechanics Publ and Elsevier Appl. Science.
Mitchell, M. 1996: *An introduction to genetic algorithms.* Cambridge, Massachusetts: The MIT Press.
Nishimura N.; Kobayashi S. 1991: A boundary integral equation method for an inverse problem related to crack detection. *Intern. Journal for Numerical Methods in Engineering*, **32**, 1371–1387.
Oeljeklaus, M.; Natke, H.G. 1996: Parallel interval algorithm for parameter identification in the frequency domain. *Inverse Problems in Engineering*, **3**, 305–325.
Oishi, A.; Yamada, K.; Yoshimura, A.; Yagawa G. 1995: Quantitative nondestructive evaluation with ultrasonic method using neural networks and computational mechanics. *Computational Mechanics* **15**, 521–533.
Rajeev, S.; Krishnamoorthy, C.S. 1992: Discrete optimization of structures using genetic algorithms. *ASCE J. of Struct. Engng.*, **118(5)**, 1233–1250.
Rajeev, S.; Krishnamoorthy, C.S. 1997: Genetic algorithms- based methodologies for design optimization of trusses. *ASCE J. of Struct. Engng.*, **123(3)**, 350–358.
Le Riche, R.; Haftka, R.T. 1993: Optimization of laminate stacking se-

quence for buckling load maximization by genetic algorithm. *AIAA Journal*, **31(5)**, 951–956.
Schnur, D.S.; Zabaras, N. 1992: An inverse method for determining elastic material properties and a material interface. *Int. J. for Num. Methods in Engineering*, **33**, 2039–2057.
Stavroulakis, G.E.; Antes, H. 1997: Nondestructive elastostatic identification of unilateral cracks through BEM and Neural Networks. *Computational Mechanics* **20(5)**, 439-451.
Stavroulakis, G.E.; Antes, H. 1998: Neural crack identification in steady state elastodynamics. *Computer Methods in Applied Mechanics and Engineering* (in press)
Tanaka, M.; Masuda, Y. 1986: An integral equation approach to inverse problems in structural mechanics. In: *Computational Mechanics 86*, Vol. 2, Eds. G. Yagawa, S.N. Atluri, pp. XI–15, XI–24, Springer.
Tanaka, M.; Nakamura, M.; Nakano, T.; Ishikawa, H. 1991: Identification of defects by the elastodynamic boundary element method using noisy additional information. In: "Boundary Elements XIII", Eds. C.A. Brebbia, G.S. Gipson, pp. 799–810, Computational Mechanics Publ. and Elsevier Appl. Science.
Tosaka, N.; Utani, A.; Takahashi, H. 1995: Unknown defect identification in elastic field by boundary element method with filtering procedure, *Engineering Analysis with Boundary Elements*, **15** 207–215.
Weijiang, C.; Chuntu, L. 1996: A BIEM optimization method for fracture dynamics inverse problem. *Acta Mechanica Sinica*, **12(3)**, 263–271.
Yagawa, G.; Okuda, H. 1996: Neural networks in computational mechanics. *Archives of Computational Methods in Engineering* **3(4)** 435-512.
Yoshimura, S.; Matsuda, A.; Yagawa, G. 1996: New regularization by transformation for neural network based inverse analyses and its application to structure identification, *Intern. Journal of Numerical Methods in Engineering* **39** 3953–3968.
Zabaras, N.; Morellas, V.; Schnur, D. 1989: A spatially regularized solution of inverse elasticity problems using the boundary element method. *Comm. Appl. Numerical Methods*, **5** 547–553.

Figure captions

Fig. 1: Configuration of a plate with two flaws.

Fig. 2: Undeformed and deformed configuration under static loading for a plate with three flaws.

Fig. 3: (a) Plot of the error function and (b) of its logarithmic version for several cyclical flaws of diameter equal to 0.1. Comparison with a flaw at point $(5.0, 5.0)$, for static excitation.

Fig. 4: Two-flaw identification using static data.
(a) Center of the first flaw,
(b) center of the second flaw,
(c) diameter of the two flaws and
(d) error function plot.

Fig. 5: One-flaw identification using static data and the two–flaw model.

Fig. 6: Undeformed and deformed configuration (magnified by a factor of 10.0) under harmonic dynamic loading for a plate with three flaws. Excitation frequencies equal to 5.0, 10.0, 15.0 and 20.0.

Fig. 7: (a) Plot of the error function and (b) of its logarithmic version for several cyclical flaws of diameter equal to 0.5. Comparison with a flaw at $(4.0, 4.0)$ for dynamic excitation.

Fig. 8: Plot of the error function (cf., Fig. 7a). Effect of using only one excitation. Excitation frequencies:
(a) 5.0, (b) 10.0, (c) 15.0 and (d) 20.0.

Fig. 9: Plot of the error function (cf., Fig. 7a). Effect of using different excitation/ measurement data. Single excitation frequency 10.0.
(a) Ox loading and Ox measurement,
(b) Ox loading and Oy measurement,
(c) Oy loading and Ox measurement, and
(d) Oy loading and Oy measurement.

Fig. 10: One-flaw elastodynamic identification problem by genetic optimization.
(a) Initial and final flaw population (center of flaw) and
(b) history of the maximum and minimum fitness values through the generations.

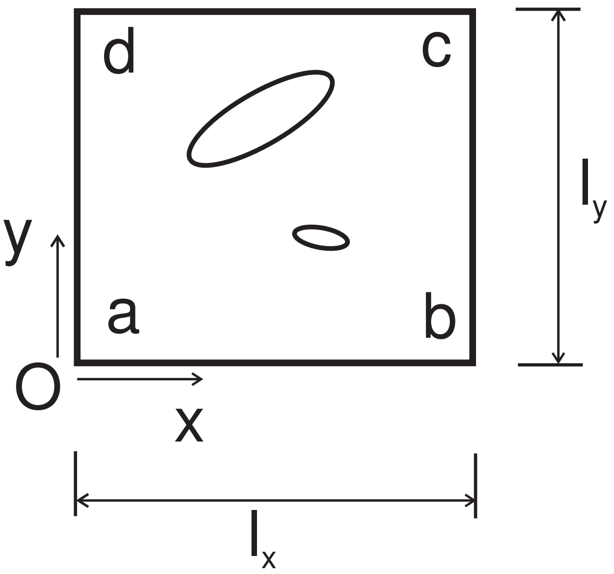

Figure 1: Configuration of a plate with two flaws.

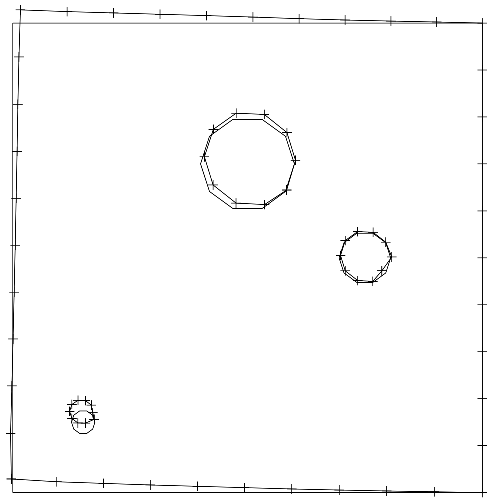

Figure 2: Undeformed and deformed configuration under static loading for a plate with three flaws.

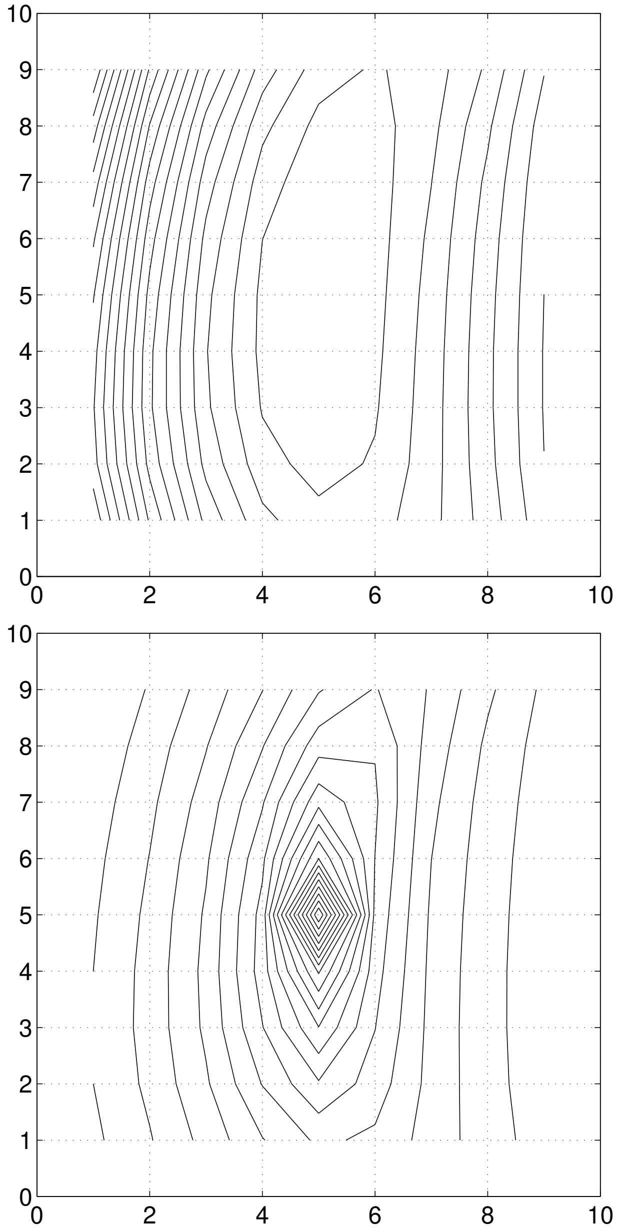

Figure 3: (a) Plot of the error function and (b) of its logarithmic version for several cyclical flaws of diameter equal to *0.1*. Comparison with a flaw at point *(5.0, 5.0)*, for static excitation.

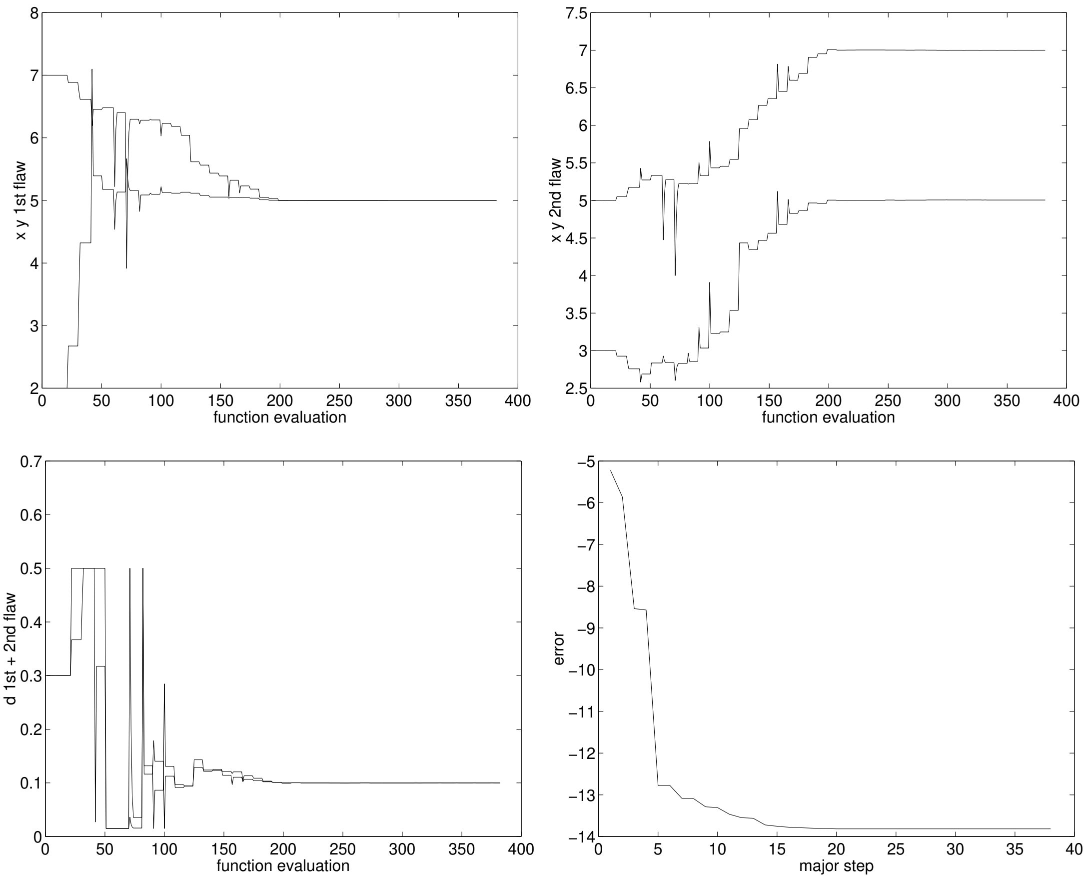

Figure 4: Two-flaw identification using static data. (a) Center of the first flaw, (b) center of the second flaw, (c) diameter of the two flaws and (d) error function plot.

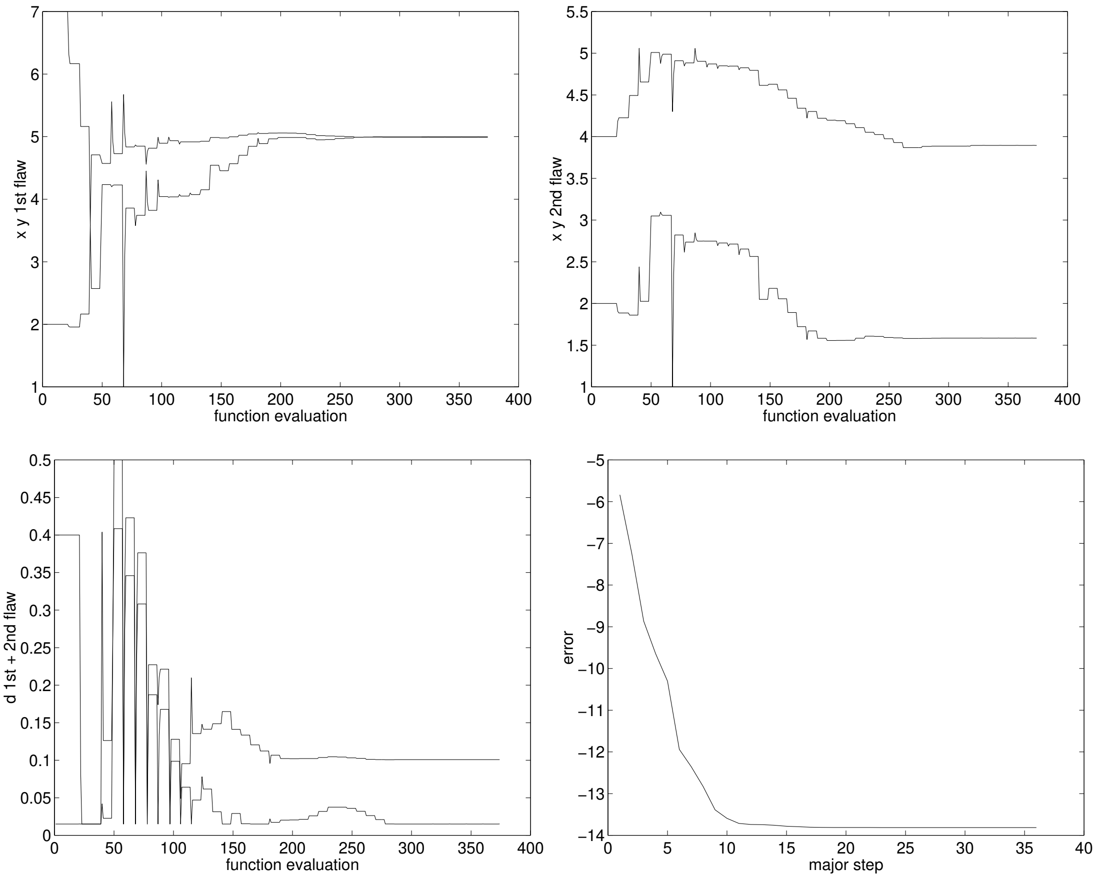

Figure 5: One-flaw identification using static data and the two-flaw model.

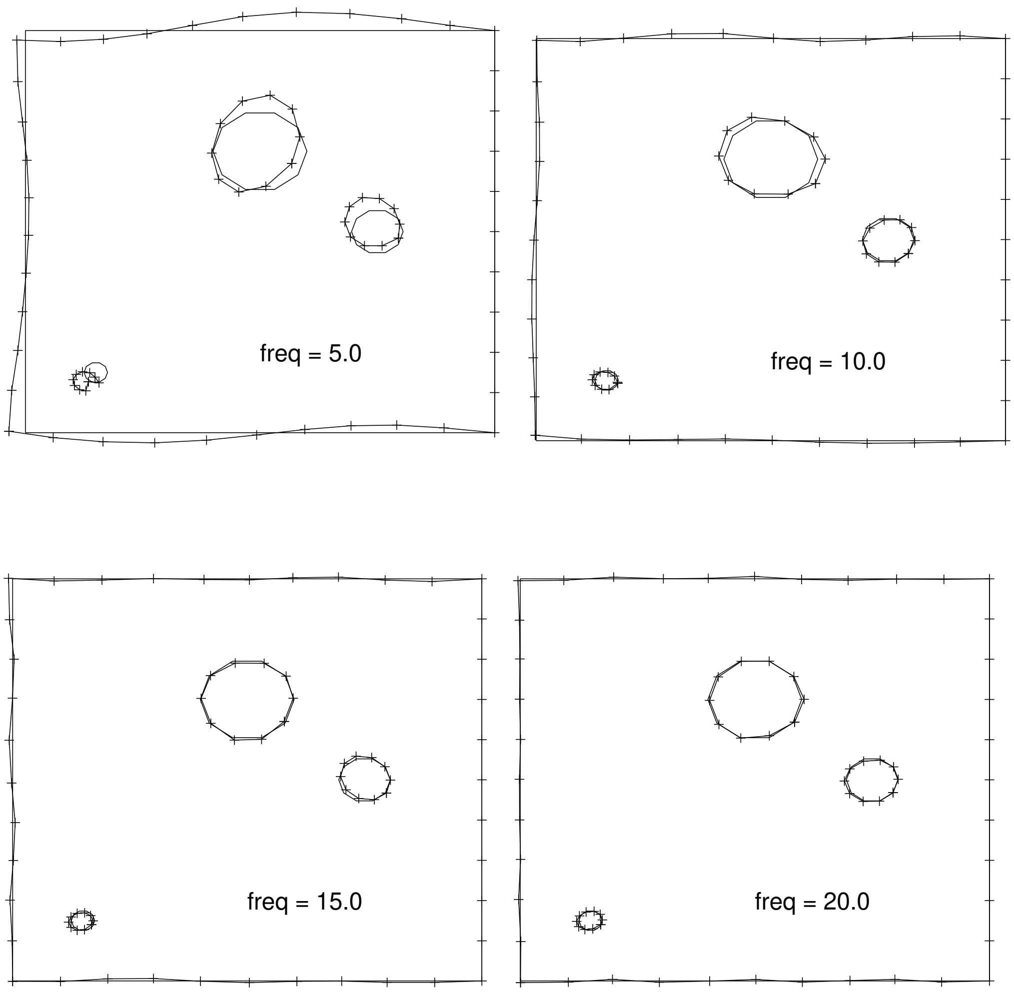

Figure 6: Undeformed and deformed configuration (magnified by a factor of *10.0*) under harmonic dynamic loading for a plate with three flaws. Excitation frequencies equal to *5.0*, *10.0*, *15.0* and *20.0*.

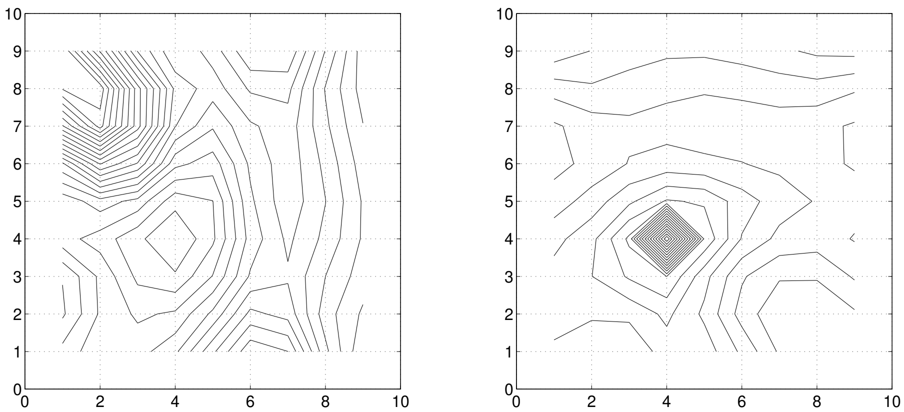

Figure 7: (a) Plot of the error function and (b) of its logarithmic version for several cyclical flaws of diameter equal to *0.5*. Comparison with a flaw at *(4.0, 4.0)* for dynamic excitation.

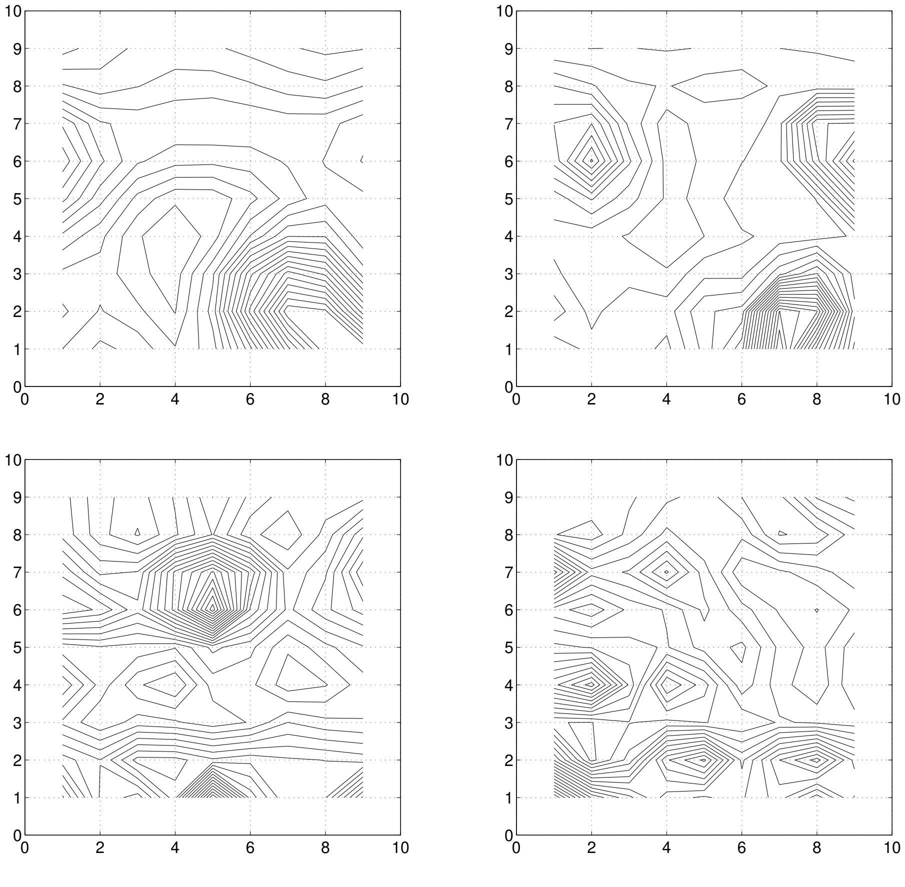

Figure 8: Plot of the error function (cf., Fig. 7a). Effect of using only one excitation. Excitation frequencies: (a) *5.0*, (b) *10.0*, (c) *15.0* and (d) *20.0*.

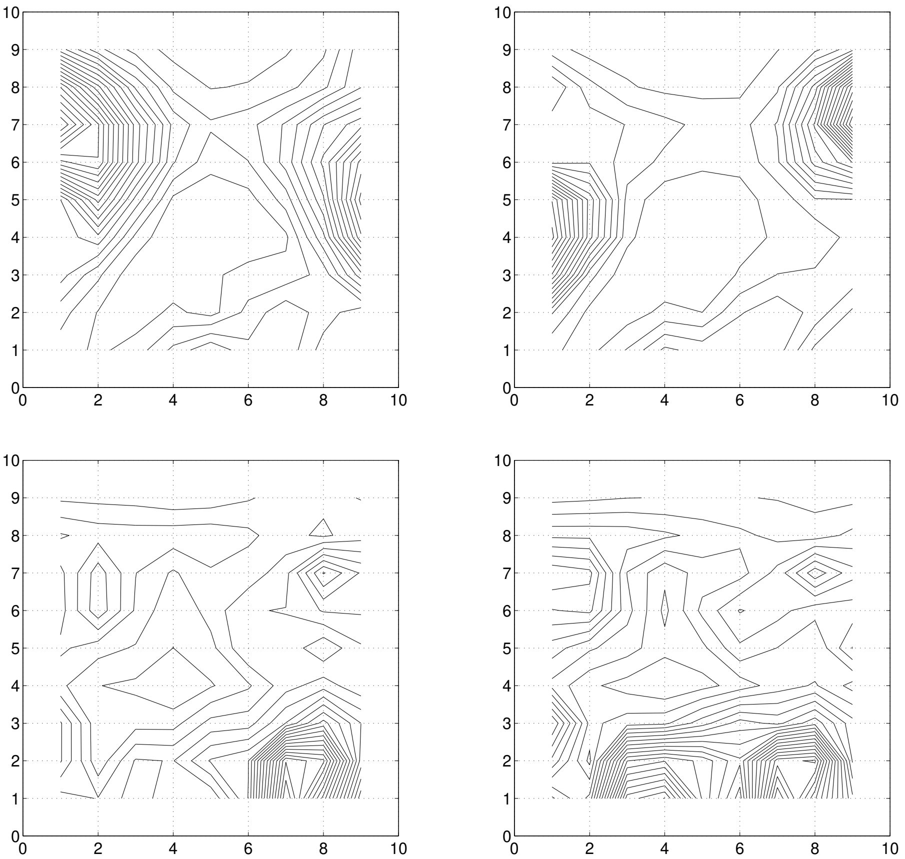

Figure 9: Plot of the error function (cf., Fig. 7a). Effect of using different excitation/ measurement data. Single excitation frequency *10.0*. (a) Ox loading and Ox measurement, (b) Ox loading and Oy measurement, (c) Oy loading and Ox measurement, and (d) Oy loading and Oy measurement.

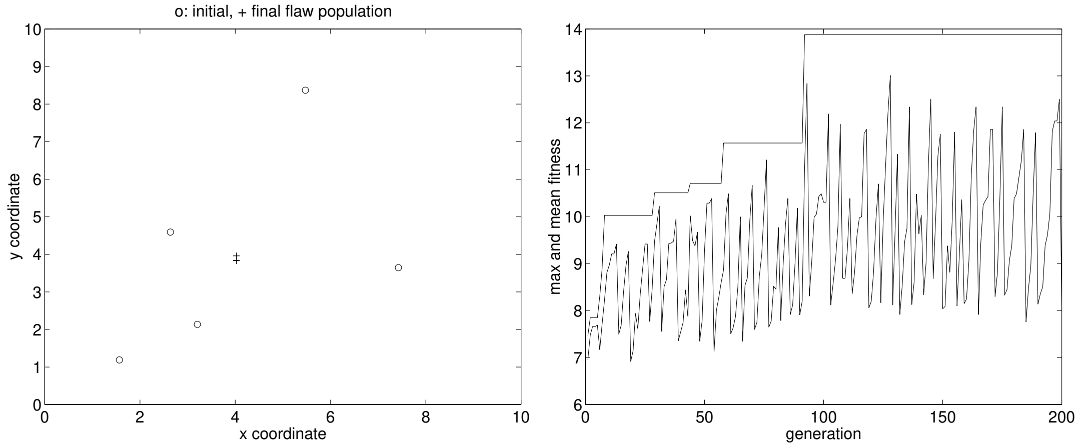

Figure 10: One-flaw elastodynamic identification problem by genetic optimization. (a) Initial and final flaw population (center of flaw) and (b) history of the maximum and minimum fitness values through the generations.